

CONSERVATIVE SOLUTE TRANSPORT FROM SOIL TO RUNOFF FLOW IN A STEEP SLOPE AREA

Ngoc Anh Thi Nguyen^{1*}, Priana Sudjono¹, Gilang Trisna Kusuma¹, Agus Yodi Gunawan²,
Barti Setiani Muntalif¹

¹*Department of Environmental Engineering, Faculty of Civil and Environmental, Bandung Institute of Technology, Bandung 40132, Indonesia*

²*Industrial and Financial Mathematics Research Group, Faculty of Mathematics and Natural Sciences, Bandung Institute of Technology, Bandung 40132, Indonesia*

(Received: June 2018 / Revised: August 2018 / Accepted: December 2018)

ABSTRACT

Solute transport through soil is the major source of nonpoint pollution. Overland flow development in a steep slope area is a complex and nonlinear system that can be influenced by infiltration excess, saturation excess, and subsurface flow. Variations in rainfall intensity, slope, and land cover can also affect the soil moisture dynamics leading to overland flow formation. This study aims to define the dominant mechanism of runoff generation in a steep slope area. A computational model is developed to estimate the quantities of runoff flow and salinity concentration in soil layers at different depths. For this purpose, field research was conducted with several rainfall heights and land cover types in an area of 57 m² with average slope of 46.7%. Field experiments indicated that the surface and subsurface flows in a soil depth of up to 30 cm were not dominant mechanisms in clay soil with steep slope even under high rainfall intensity. The output of the flow quantitative model showed that overland flow generation in the field plot was dominated by the saturation excess mechanism. The natural grass plot showed the lowest overland flow percentage; by contrast, removed grass and without grass plots showed percentages of 19.49% and 19.18% for rainfall height of 24.9 and 21.8 mm, respectively. Land cover was identified as an important factor affecting runoff generation. The output of the solute transport model for rainfall height of 24.9 mm with salt addition indicated that natural grass and removed grass plots had the lowest salinity concentrations of 55.45 and 33.62 ppm, respectively. Salinity transport was slowest on the natural grass plot, and it started only 45–50 min after artificial rain was applied.

Keywords: Overland flow; Rainfall intensity; Soil characteristics; Solute transport; Steep slope area

1. INTRODUCTION

Solute transport from soil through overland flow is a major source of nonpoint pollutants in receiving surface water bodies. Salinity is the main problem that occurs in almost all irrigated areas and even in some non-irrigated areas such as grasslands and open fields (Szabolcs, 2011). Studies found that up to 20 million hectares of soil in Southeast Asia is affected by salinity. Salinity problems in tropical countries cause soil characteristics to deteriorate, increase soil erodibility, and inhibit plant growth (Kovda & Szabolcs, 1979; Szabolcs, 2011). The Food and

*Corresponding author's email: ngoc.anh@students.itb.ac.id, Tel. +62-85-861444235
Permalink/DOI: <https://doi.org/10.14716/ijtech.v9i7.2458>

Agriculture Organization (FAO) and the United Nations Educational, Scientific, and Cultural Organization (UNESCO) estimate that many existing irrigation systems worldwide are affected by secondary salinization, alkalization, and waterlogging. These phenomena are seen in both old and newly irrigated areas. Salinization is a global environmental phenomenon that significantly decreases the quality of water resources; nonetheless, it has not yet attracted much global attention (Gibbs et al., 2011).

The movement of overland flow directly affects the soil salinity. Xu and Shao (2002) stated that salinization is closely related to hydrological processes that occur on the soil surface and in groundwater, because the movement of water is a very important factor in the transfer of salt as a conservative material. In steep-slope areas, the theory of overland flow is based on differentiation between overland flow generation from excessive infiltration and excessive saturation and subsurface flow (Ameli et al., 2015). Overland flow is harder to define precisely than in-channel flow, and the use of hydraulic procedures in predicting overland flow and its characterization has limitations (Kirkby, 1978). It is unstable and varies spatially as it arises from rainwater and decreases due to infiltration; these two processes are not constant over time and space. Studies thus far have mainly focused on a basis for quantifying the transformation from rainfall to overland flow.

Alaoui et al. (2011) indicated that hillslopes with higher clay content produced higher overland flow volumes than hillslopes in forest areas. Land cover also influences overland flow formation in steep slope areas, where soil with less dense vegetation tended to show a higher overland flow formation rate compared to soil with denser natural vegetation cover (Qing-Xue et al., 2013). Zhao et al. (2015) found that rainfall intensity, slope, and land cover types can affect soil moisture dynamics and lead to overland flow formation. A detailed study of the overland flow formation mechanism in steep slope areas is required to establish a runoff model that researchers can use to determine appropriate management practices to reduce the amount of discharge runoff and the relocation of solutes via surface runoff, especially from steep slopes to water bodies.

Therefore, field research was conducted in a steep-slope catchment having uniform slope of 46.7%. In order to define the runoff generation mechanism based on the distribution of conservative matter, results of several scenarios on rain intensity, soil characteristics, and vegetation density were evaluated.

2. METHODS

2.1. Field Measurement and Data Requirement

Field research was conducted by testing overland flow generation on soil with area of $\sim 57 \text{ m}^2$ (width: 6 m, length: 9.5 m) and average slope of 46.7%. The soil plot was divided into three types of land cover: natural grass (NG), removed grass (RG), and without grass (WG). Artificial rainfall was provided to examine the runoff mechanism. Figure 1 shows a schematic plan of the research area. Rainfall was supplied through the pipe system of a rainfall simulator over the soil surface, as shown in Figure 2. The flow of the water source was measured before supplying rain to determine the volume of water used and then converted to rainfall height per unit time. Two scenarios of rain intensity 21.8 mm/hour and 24.9 mm/hour were applied in the field research to observe runoff flow and solute transport through the runoff. A crystalline salt solution was added only on 24.9 mm/hour rainfall scenario. In which salt solution had poured on upper part of each soil plots before rain was applied. Soil physical characteristics such as saturated hydraulic conductivity (K_{sat}), moisture, and electrical conductivity (EC) were measured. For soil depth of 10–30 cm, K_{sat} was measured using a constant head permeameter (Talsma & Hallam, 1980). For soil depth of 0–10cm, K_{sat} was measured by inserting a ring infiltrometer

into the soil (Youngs, 1987). Moisture and EC were measured using a moisture meter and direct EC meter, respectively, 0, 60, and 120 min into each rainfall event. Changes in soil moisture and EC values were used as indicators of runoff and salt transport in soil layers with depths of 0–10, 10–20, and 20–30 cm.

EC is used as a unit for electrical conductivity measurements in water or other liquids. In some conductivity meters, conductivity values are shown in “EC” units, where 1 EC corresponds to 1 mS/cm. Parts per million (ppm) indicates the number of units of a particle per million units of a fluid. These units are interconvertible as 1 mS/cm = 640 ppm (ppm₆₄₀) (Easy calculator; Unit Converter, 2017).

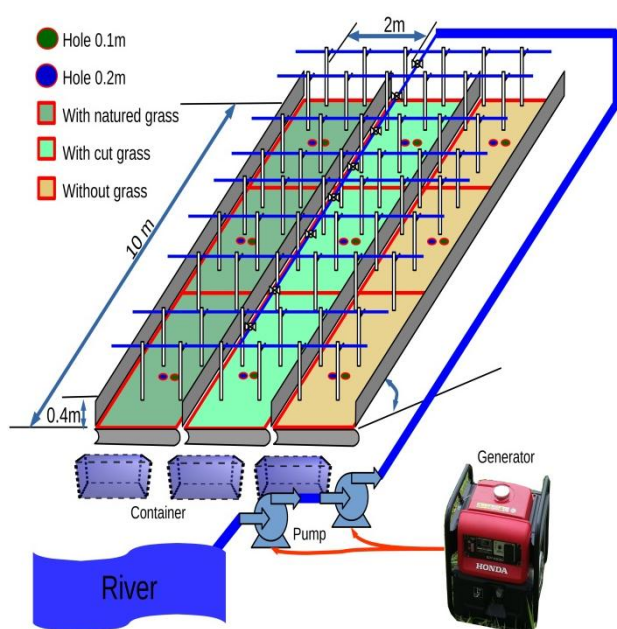


Figure 1 Experimental design of plot area used in study



Figure 2 Pipe system for supplying artificial rainfall

2.2. Quantity Formulation of Overland Flow Generation on Steep-Sloped Area

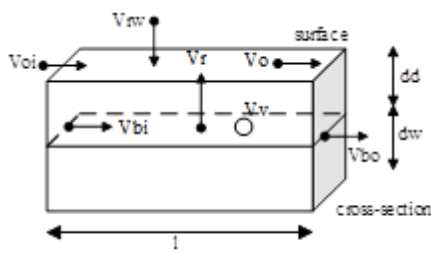
A water balance study was used for simulating surface hydrological processes in the same way as in previous studies (Wu et al., 2001; Hayashi et al., 2008).

$$\Delta V^{in} = \Delta V^{out} + \Delta V^{storage} \tag{1}$$

Equation 1 for each segment, as shown in Figure 3, can be developed based on Sudjono (1995) with the assumption that the overland flow rate is constant.

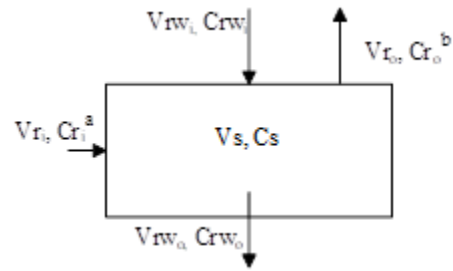
$$\Delta V_{rw} + \Delta V_{bi} + \Delta V_{oi} + \Delta V_{ri} = \Delta V_v + \Delta V_{bo} + \Delta V_r + \Delta V_o \tag{2}$$

where V_{rw} is the volume of rainfall on the segment; V_{bi} , the volume of subsurface inflow to the segment; V_{bo} , the volume of subsurface outflow from the segment; V_v , the volume of rainfall retained in the segment; V_{oi} , the volume of incoming overland flow; V_o , the volume of overland flow produced by the segment; V_{ri} , the volume of incoming return flow; and V_r , the volume of return flow from the segment.



Each segment with width ($b=2$ m), length ($l=3.167$ m), and depth ($d_{seg}=10$ cm = 0.1 m) divided into d_d (depth of dry soil solid) and d_w (depth of soil water)

Figure 3 Scheme of constituent components of the volume segment in the model



(a) additional components for segments [2,1] and [3,1]; (b) an additional component for the segment if soil becomes saturated

Figure 4 Components in the calculation of the conservative solute concentration of each segment

The return flow component is made opposite to the incoming rainwater to simplify the calculation iteration of each segment and layer in the model. If the rainfall volume entering the layer exceeds the available void volume, then a return flow to the upper layer is formed. In each segment, the calculation was started from the lowest depth (20–30 cm). If the rainfall volume entering the layer exceeds the available void volume, a return flow will appear in the 10–20 cm layer and so on up to the upper 0–10 cm layer. If the surface layer (0–10 cm) becomes saturated, V_r will contribute to the rainwater volume to the next segment shown in the longitudinal model scheme in the plot of the research area (Figure 5).

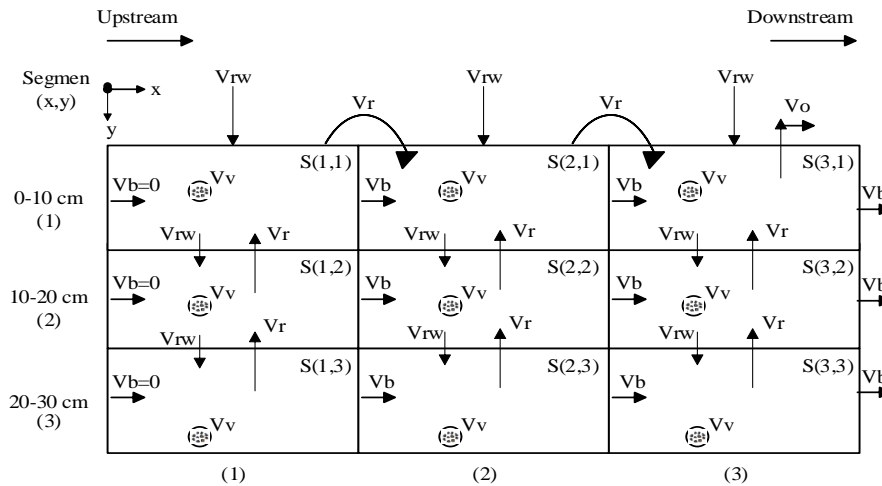


Figure 5 Cross-sectional segmentation of model from research plot

The amount of rainfall held in a segment depends on the change in soil pores or voids in the segment (ΔV_v), which in turn is affected by the porosity (p), depth of dry layer (d_d), and surface area of segment (A).

$$\Delta V_v = p \times \Delta d_d \times A \tag{3}$$

where A can be calculated based on the width b and length l of each segment as in Equation 4:

$$A = b \times l \tag{4}$$

and d_d can be calculated based on the wet depth (d_w) of that segment, as shown in Figure 3, with the assumption that d_w is proportional to soil moisture.

The return flow volume is the difference between the rainwater volume and the void volume in the segment. V_r formation occurs when the initial available void volume is fully charged, giving Equation 5:

$$V_r = V_{v\ initial} - V_{rw} \tag{5}$$

If the catchment area has not reached saturation before rainfall starts, then when rainfall does start, part of the rainwater fills the soil pores and the rest stays on the leaves and trees. Therefore, the amount of rainfall reaching the soil surface decreases with the coefficient of rainfall losses (C_d).

$$\Delta V_{rw} = i(t) \times A \times \Delta t \times C_d \tag{6}$$

where $i(t)$ is the rain intensity ([L]/[T]); A , the surface area of the segment; and Δt , the time step for the calculation.

The rainwater volume received by each plot varies according to the type of land cover, where less vegetation cover results in a segment receiving higher rainfall volume. C_d was assumed to be 0.6, 0.7, and 0.85 for the NG, RG, and WG plots, respectively.

The subsurface flow volume is given by Darcy’s law with the assumption that the hydraulic gradient of the water surface in the permeable layer is equivalent to the slope (s) as:

$$\Delta V_b = q_b \times \Delta t = k \times \Delta a \times s \times \Delta t \tag{7}$$

The change in segment area Δa is given as the product of the segment width (b) and saturated layer (d_w) as:

$$\Delta a = b \times \Delta d_w \tag{8}$$

The overland flow change (ΔV_o) is a part of the amount of exiting water (ΔV_{out}) that can be determined using the overland flow and timestep (Δt) as:

$$\Delta V_o = q_o \times \Delta t \tag{9}$$

Equation 2 can be rewritten as:

$$\Delta V_v = \Delta V_{rw} + \Delta V_{bi} + \Delta V_{oi} + \Delta V_{ri} - \Delta V_{bo} - \Delta V_r - \Delta V_o \tag{10}$$

This equation gives the rainfall volume needed to completely fill the segment when it is not saturated, that is, $\Delta V_o = 0$, $\Delta V_r = 0$, $\Delta V_{oi} = 0$, and $\Delta V_{ri} = 0$. Therefore, Equation 10 can be rewritten as:

$$\Delta V_v = \Delta V_{rw} + \Delta V_{bi} - \Delta V_{bo} \tag{11}$$

If the hydraulic conductivity k was assumed to be constant in each segment, then the incoming subsurface V_{bi} and exiting subsurface V_{bo} flow of the segment can be equated. With this assumption, $\Delta V_b = 0$, and therefore, $\Delta V_v = \Delta V_{rw}$. From Equation 5, on the shallower layer of the segment, the rainfall component (V_{rw}) is the return flow component from the deeper segment of the same row (V_r).

Equations 1–11 were used in the flow quantitative model.

2.3. Conservative Solute Transport Model Development

The salinity concentration in each soil layer was measured using a direct EC meter before rainfall simulation, and this value was then converted from units of mS/cm to ppm. Salt spread on the top segment in the form of a mixture concentration of 0.166 M (5910 ppm).

Various factors play a role in determining the salinity concentration in a segment (Figure 4): water volume V_s and initial salt concentration C_s in the segment; rainwater volume V_{rwo} and salt concentration C_{rwo} output from this segment to the next segment; and return flow volume V_{ri} and V_{ro} and salt concentration C_{ri} and C_{ro} if the soil has become saturated.

A conservative solute transport model was developed using the various parameters of the flow quantitative model among the segments with the assumption that the solute concentration in each segment was completely diluted. Therefore, the solute concentration in each segment can be calculated as:

$$C_{s \text{ final}} = \frac{[(C_{input} \cdot V_{input}) - (C_{output} \cdot V_{output}) + (C_{s \text{ initial}} \cdot V_{s \text{ initial}})]}{V_{input} - V_{output} + V_{s \text{ initial}}} \quad (12)$$

where the incoming volume and concentration might be from rainfall entering the segment or return flow from the segment below, and a return flow is produced if the segment becomes saturated.

3. RESULTS AND DISCUSSION

3.1. Measurement of Soil Characteristics, Moisture, and Electric Conductivity

The K_{sat} values measured in the three layers—0.00108 m/day (0–10 cm), 0.00104 m/day (10–20 cm), and 0.00087 m/day (20–30 cm)—were considered very small. K_{sat} in the shallower layer of soil (0–10 cm) was greater than that in the other two layers (10–20 and 20–30 cm). Therefore, water entering the soil vertically moved slower after passing the 0–10 cm layer. We compared the K_{sat} values with those reported by Smedema and Rycroft (1983) based on the relationship between soil hydraulic conductivity and soil texture. The 0–10 cm layer in the field was classified as clay soil that is porous due to weathering and overgrown vegetation, and the 10–30 cm layer was classified as denser clay soil. The field research plot has high water holding capacity, low water infiltrability into soil, and slow vertical movement of water into soil. Laboratory analysis results supported these findings, and the plot was classified as clay soil based on USDA textural triangle classification.

Under high intensity of artificial rainfall (24.9 and 21.8 mm/h), overland flow from surface or subsurface flows was not observed up to a depth of 30 cm in soil. This may be because surface and subsurface flows from 0–30 cm were not the dominant mechanism in the field research plot. Soil can hold rainwater before it infiltrates the deeper soil layer below a depth of 30 cm; furthermore, the plot length (9.5 m) is not enough to establish a return flow. The runoff generation mechanism cannot be observed visually; however, it is evidenced by the soil moisture content. Therefore, soil moisture data during rainfall can be used in a mathematical model to quantify the water content and salinity concentration in soil layers.

3.2. Mathematical Model of Overland Flow Formation

The low K_{sat} value influenced V_b in the model and caused V_r to form from the decreasing void volume (V_v), according to Equation 5, until the saturation excess phenomenon was seen, indicating domination of overland flow formation.

The output of the flow quantitative model indicated the distribution of rainfall volume entering each segment (Table 1). In the NG plot, the percentage of overland flow formation tended to be

the lowest for both rainfall heights. In the RG and WG plots, the percentage of overland flow formation increased up to 30.56% and 75.31%, respectively, for the lower rainfall height. Therefore, vegetation density may affect the amount of runoff volume produced by the model.

Table 1 Distribution of V_{rw} in each segment

V_{rw} in segment		I = 24.9 mm/h ^a			I = 21.8 mm/h		
Segment		NG	RG	WG	NG	RG	WG
Upper		0.0946	0.1104	0.1340	0.0828	0.0966	0.1174
Middle		0.0946	0.1104	0.1340	0.0828	0.0966	0.1174
Lower		0.0946	0.1104	0.1340	0.0828	0.0966	0.1174
Total V_{rw} (m ³)		0.2839	0.3312	0.4021	0.2485	0.2899	0.3521
V_r distributed		Plot type			Plot type		
Segment	layer (cm)	NG	RG	WG	NG	RG	WG
Upper	20–30	0.0044	0.0450	0.0374	0.0024	0.0397	0.0356
	10–20	0.0222	0.0398	0.0309	0.0362	0.0336	0.0025
	0–10	0.364	0.0382	0.0368	0.0071	0.0401	0.0074
Middle	20–30	0.0363	0.0371	0.0026	0.0379	0.0056	0.0132
	10–20	0.0282	0.0016	0.0362	0.0062	0.0124	0.0062
	0–10	0.0344	0.0364	0.0398	0.0365	0.0074	0.0116
Lower	20–30	0.0344	0.0364	0.0398	0.0365	0.0074	0.0116
	10–20	0.0258	0.0369	0.0376	0.0301	0.0430	0.0060
	0–10	0.0037	0.0065	0.0065	0.0030	0.0049	0.0010
V_0 produced		0.0553	0.0725	0.1363	0.0415	0.0314	0.0035
Total V_{rw} (m ³)		0.2839	0.3312	0.4021	0.2485	0.2899	0.3521
% V_0		19.49%	21.90%	33.89%	19.18%	30.56%	75.31%

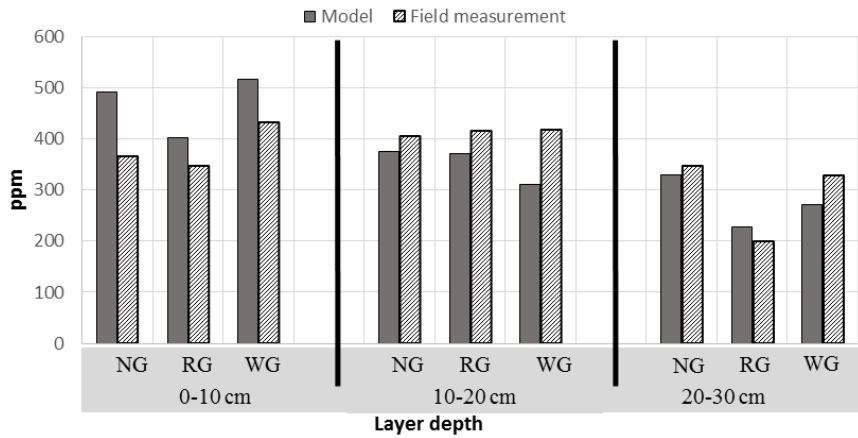
V_0 : volume of surface runoff; a) with salt addition
 NG: natural grass, RG: removed grass, WG: without grass

All three types of soil plots showed higher overland flow percentage at rainfall intensity of 21.8 mm/h than at 24.9 mm/h. The higher overland flow percentage in RG and WG plots under lower rainfall intensity was affected by the uneven distribution of incoming rainfall volume entering each segment and layer that in turn was caused by the difference in saturation level in each soil segment. Therefore, rainfall intensity might not be an important factor affecting the amount of runoff volume produced by the model in clay soil and steep slope areas.

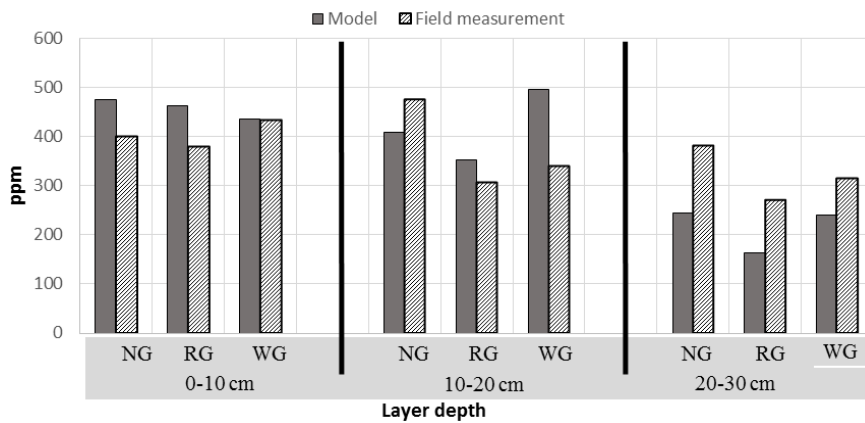
3.3. Calculation of Salinity Concentration based on Model Output with Field Measurement Data

Based on the volumetric components determined from the flow quantitative model, the salinity concentration after 60 min of artificial rainfall in the output model and field measurement was the highest in the 0–10 cm layer. In this layer, the WG plot showed the highest concentration. The higher concentration in the surface layer was caused by the distribution of the conservative solute poured on this layer in the upper segments.

Generally, the model output and field measurement showed similar patterns, especially for rainfall height of 24.9 mm as shown in Figure 6a. The surface layer (0–10 cm) showed a significant difference between the model output and field measurement for rainfall height of 24.9 mm; the average salinity concentration was closer to the field measurement for rainfall height of 21.8 mm, as shown in Figure 6b. These results indicate that complete dilution did not occur in the segment. For the 10–20 and 20–30 cm layers, the average model output concentration showed smaller error for rainfall height of 24.9 mm than for rainfall height of 21.8 mm.



(a) rainfall height of 24.9 mm with salt addition



(b) rainfall height of 21.8 mm

Figure 6 Comparison of average salinity concentration in soil layer between model output and field measurement

This phenomenon is attributed to the uneven distribution of salt in each plot in the field across the upper segments, result in the model output in the surface layer (0–10 cm) being less accurate for rainfall height of 24.9 mm than for rainfall height of 21.8 mm.

Figure 7 shows the distribution of salinity concentrations in the runoff from each plot.

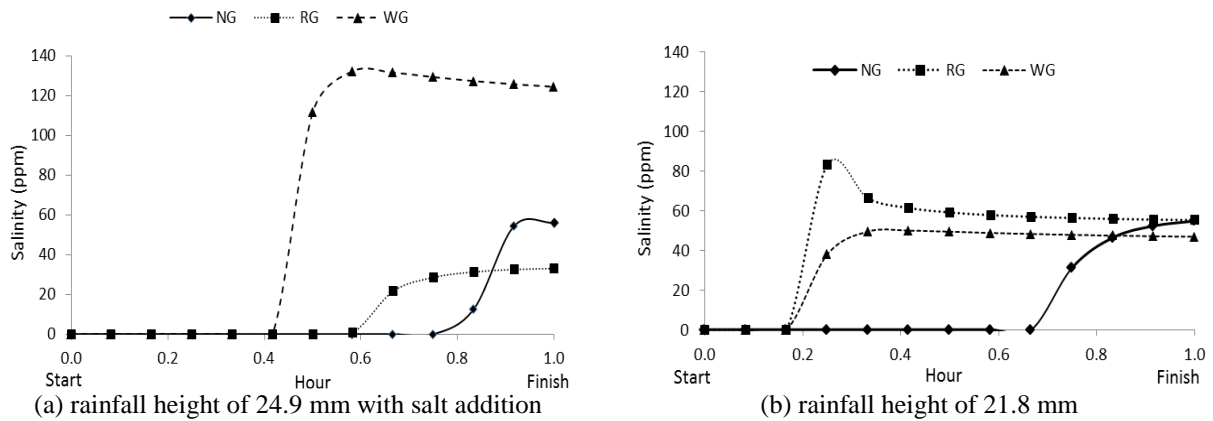


Figure 7 Transport of salinity concentration in overland flow under different rainfall intensities

For rainfall height of 24.9 mm, the WG plot showed the highest salinity concentration of 124.43 ppm in the runoff; the NG and RG plots showed lower salinity concentration of 56.04 and 33.05 ppm, respectively. For lower rainfall height of 21.8 mm, the RG plot showed the highest salinity concentration of 83.00 ppm; the NG and WG plots showed lower salinity concentration of 54.71 and 49.91 ppm, respectively. The high and low salinity concentration in overland flow produced from the WG plot under high and low rainfall, respectively, indicated that salinity might be transported easily in the surface runoff of a bare plot under high rainfall. Furthermore, vegetation cover might not have an important effect on salinity movement under low rainfall.

The salinity concentration increased more stably in the RG and WG plots than in the NG plot under both rainfall heights. Under higher rainfall, salinity emerged at the 50th, 40th, and 30th min in NG, RG, and WG, respectively. Under lower rainfall, salinity emerged in the runoff at the 45th min in NG and earlier than the 15th min in RG and WG.

4. CONCLUSION

The proposed field experiment design, although difficult to perform, provides a general structure for analyzing runoff flow and a better understanding of the main flow mechanism in steep-slope areas. In clay soil in a steep slope area, surface or subsurface flows were not observed below depths of 0–30 cm in soil even under high artificial rainfall intensity. This indicates that surface and subsurface flows at depths of 0–30 cm were not the dominant mechanism in soil with high water-holding capacity. Rainwater can be held in soil or can infiltrate the deeper soil layer. Land cover might be a more important factor than rainfall intensity in clay soil for runoff flow generation. This study proposes a suitable computational model to estimate runoff generation and salinity concentration based on moisture dynamics if runoff cannot be observed in the discharge. The output of the flow generation model for each plot indicates that overland flow generation on a steep slope plot might be dominated by saturation excess, whereas a Natural grass plot shows the lowest overland flow generation percentage compared to Removed grass and Without grass plots. For higher rainfall height of 24.9 mm with salt addition, the salinity concentration in the WG plot was the highest at 124.43 ppm compared to 56.04 and 33.05 ppm for the Natural grass and Removed grass plots, respectively. Furthermore, salinity was detected only after 45 and 50 min of low and high rainfall, respectively, in the NG plot.

5. ACKNOWLEDGEMENT

The authors are grateful to the Bandung Institute of Technology and wish to acknowledge the Financial Support from AUN-Seed Net Scholarship 2016. We would like to thank everyone else who has supported this research.

6. REFERENCES

- Alaoui, A., Caduff, U., Gerke, H.H., Weingartner, H., 2011. A Preferential Flow Effects on Infiltration and Runoff in Grassland and Forest Soils. *Vadose Zone Journal*, Volume 10 (1), pp. 367–377
- Ameli, A.A., McDonnell, J.R., Craig, J.R., 2015. Are All Runoff Processes the Same? Numerical Experiments Comparing a Darcy-Richards Solver to and Overland Flow-base Approach for Subsurface Storm Runoff Simulation. *Water Resources Research*, Volume 51(12), pp. 10008–10028
- Easy Calculator, 2017. Available Online at <https://www.easycalculation.com/unit-conversion/microsiemens-ppm-conversion.php>, Accessed on September 8, 2017

- Gibbs, M.S., Maier, H.R., Dandy, G.C., 2011. Runoff and Salt Transport Modelling to Maximize Environmental Outcomes in the Upper South East of South Australia. *In: 19th International Congress on Modelling and Simulation. Modelling and Simulation Society of Australia and New Zealand (MODSIM2011)*, Chan, F., Marinova, D., Anderssen, R.S. (eds), pp. 3847–3853. ISBN: 978-0-9872143-1-7. <https://www.mssanz.org.au/modsim2011/19/gibbs.pdf>
- Hayashi, S., Murakami, S., Kai-Qin, X., Watanabe, M., Bao-Hua, X., 2008. Daily Runoff Simulation by an Integrated Catchment Model in the Middle and Lower Regions of the Changjiang Basin, China. *Journal of Hydrologic Engineering*, Volume 13(9), pp. 846–862
- Kirkby, M.J., 1978. *Hillslope Hydrology*. Wiley & Sons Ltd.: Norwich
- Kovda, V.A., Szabolcs, I., 1979. Modeling of Soil Salinization and Alkalinization. *Agrokemia es Talajtan*, 28, Suppl.
- Qing-Xue, X., Tian-Wei, W., Chong-Fa, C., Zhao-Xia, L., Zhi-Hua, S., Rong-Jie, F., 2013. Responses of Runoff and Soil Erosion to Vegetation Removal and Tillage on Steep Lands. *Pedosphere*, Volume 23(4), pp. 532–541
- Smedema, L.K., Rycroft, D.W., 1983. *Land Drainage: Planning and Design of Agricultural Drainage Systems*. Batsford: London
- Sudjono, P., 1995. A Mathematical Concept of Runoff Prediction Model for Small Tropical Catchment Areas. *Water Science Technology*, Volume 31(9), pp. 27–36
- Szabolcs, I., 2011. Soil Salinity and Sodicity as Particular Plant/Crop Stress Factors. *In: Handbook of Plant and Crop Stress*, 3rd Edition, Pessarakli, M., (ed.), CRC Press, Taylor & Francis Group, Boca Raton, Florida, USA, pp. 3–21
- Talsma, T., Hallam, P.M., 1980. Hydraulic Conductivity Measurement of Forest Catchments. *Australian Journal of Soil Resources*, Volume 30, pp. 139–148
- Unit Converter, 2017. Calculators: Convert Millisiemens/Centimeter [mS/cm] and Parts per Million, 640 Scale [ppm₆₄₀]. Available Online at <https://www.translatorscafe.com/unit-converter/en/electric-conductivity/11-18/millisiemens%2Fcentimeter-parts%20per%20million%2C%20640%20scale/>, Accessed on September 8, 2017
- Wu, R-S., Sue, W-R., Chien, C-B., Chien, C-H., Lin, K-M., 2001. A Simulation Model for Investigating the Effects of Rice Paddy Fields on the Runoff Systems. *Journal of Mathematical and Computer Modelling*, Volume 33(6-7), pp. 649–658
- Xu, P., Shao, Y., 2002. A Salt-transport Model within a Land-surface Scheme for Studies of Salinization in Irrigated Areas. *Journal of Environmental Modelling & Software*, Volume 17(1), pp. 39–49
- Youngs, E.G., 1987. Estimating Hydraulic Conductivity Values from Ring Infiltrometer Measurements. *Journal of Soil Science*, Volume 38(4), pp. 623–632
- Zhao, N., Yu, F., Li, C., Zhang, L., Kiu, J., Mu, W., Wang, H., 2015. Soil Moisture Dynamics and Effects on Runoff Generation at Small Hillslope Scale. *Journal of Hydrology Engineering*, Volume 20(7), pp. 1–13